ChemComm

Accepted Manuscript

This article can be cited before page numbers have been issued, to do this please use: Q. Wang, L. L. Zhang, C. Shang, Z. Zhang and S. Dong, *Chem. Commun.*, 2016, DOI: 10.1039/C6CC00194G.

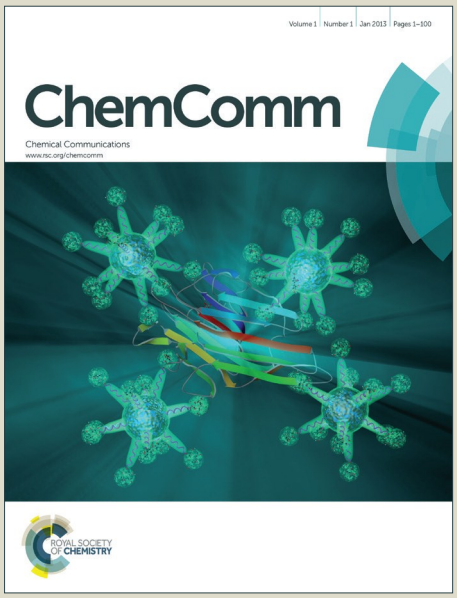

ROYAL SOCIETY OF CHEMISTRY

www.rsc.org/chemcomm

Journal Name

View Article Online
DOI: 10.1039/C6CC00194G

COMMUNICATION

Triple-enzyme mimetic activity of nickel-palladium hollow nanoparticles and their application in colorimetric biosensing of glucose

Received 00th January 20xx,
Accepted 00th January 20xx

DOI: 10.1039/x0xx00000x

www.rsc.org/

Qingqing Wang,[a, b] Lingling Zhang,[a] Changshuai Shang,[a] Zhiquan Zhang[b]* and Shaojun Dong[a]*

We demonstrate that nickel-palladium hollow nanoparticles (NiPd hNPs) exhibit triple-enzyme mimetic activity: oxidase-like activity, peroxidase-like activity and catalase-like activity. As peroxidase mimetics, the catalytic activity of NiPd hNPs was investigated in detail. On this basis, a simple glucose biosensor with a wide linear range and low detection limit was developed.

Artificial enzyme mimics have attracted much attention due to the viable merits over natural enzymes, such as easy preparation, high stability and low-price.[1] Since the first exciting discovery of ferromagnetic nanoparticles,[2] various efficient nanomaterial-based artificial enzymes (nanozymes)[3] have been developed during the past few decades. More and more nanozymes were found exhibiting oxidase, peroxidase, catalase or superoxide dismutase (SOD) mimetic activity. Very recently, a mixed valence state Ce-MOF was found exhibiting oxidase-like activity and a new approach for the detection of biothiols in serum samples was established.[4] Chen et al. reported that MFe_2O_4 (M=Mg, Ni, Cu) exhibited both peroxidase-like activity and catalase-like activity.[5] What's more, Zhang and his colleagues found a novel strategy to significantly improve the SOD mimetic activity of nanoceria with size at greater than 5 nm.[6] To date, there have been many works reported on exploiting functional nanomaterials as enzyme mimetics.[7]

Noble metals (e.g., Pd, Pt and Au)[8] and their combination with transition-metals,[7b] metal oxides[9] or carbon materials[7c, 10] have been developed rapidly because of their multi-enzyme mimetic activities, excellent catalytic properties and high chemical stability. At the same time, Pd-based nanomaterials have become promising alternative enzyme mimetics and applied widely in biological detection,[10a] immunoassay[11] and other fields. Here, we found that the NiPd hollow nanoparticles (NiPd hNPs) prepared rapidly with Ni nanospheres as sacrificial templates possessed triple-enzyme mimetic activity: oxidase-like activity, peroxidase-like activity and catalase-like activity, as shown in Scheme 1.

NiPd hNPs exhibited specific intrinsic oxidase-like activity, catalyzing the quick oxidation of TMB to display a light blue color without the presence of H_2O_2. As for the peroxidase-like activity, NiPd hNPs could catalyze the reduction of H_2O_2. In the colorimetric assay, it could catalyze the reaction of H_2O_2 and a series of organic substrates, such as TMB, ABTS and OPD to give blue, green and orange colors, respectively. On this basis, NiPd hNPs were used successfully for colorimetric biosensing of glucose by combining with glucose oxidase (GOD). Furthermore, as catalase mimics, NiPd hNPs could catalyze the decomposition reaction of H_2O_2 into oxygen and water. To sum up, we found for the first time that NiPd hNPs exhibited triple-enzyme mimetic activity.

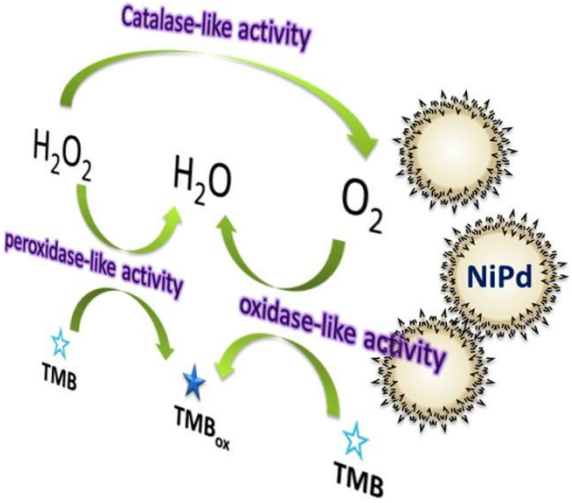

Scheme 1. Schematic presentation for triple-enzyme mimetic activity of NiPd hNPs.

[a] State Key Laboratory of Electroanalytical Chemistry, Changchun Institute of Applied Chemistry, Chinese Academy of Sciences, Changchun, 130022, P. R. China E-mail: dongsj@ciac.ac.cn (S. Dong), zzq@jlu.edu.cn (Z. Zhang). Tel: +86 431 85692886. Fax: +86 431 85689711
[b] College of Chemistry, Jilin University, Changchun, 130012, P. R. China.
† Electronic Supplementary Information (ESI) available. See DOI: 10.1039/x0xx00000x

View Article Online
DOI: 10.1039/C6CC00104C

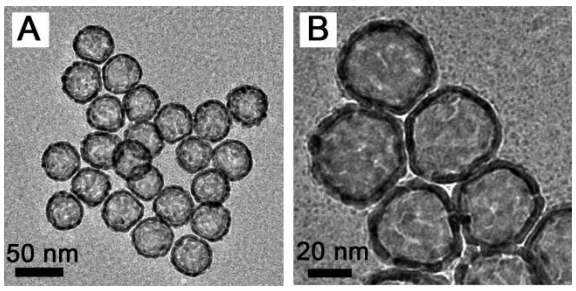

Fig. 1. TEM images of NiPd hNPs at different magnifications.

In this work, NiPd hNPs were synthesized via galvanic replacement reaction.[12] Ni nanoparticles could be gradually consumed by Pd salts because the standard reduction potential of Ni(II)/Ni is lower than that of the $PdCl_4^{2-}$/Pd couple.[13] The resulting homogeneous black NiPd hNPs dispersion was obtained with good stability and reproducibility. Fig. 1A and 1B showed the transmission electron microscopy (TEM) images of NiPd hNPs at different magnifications. It is clear that the hollow-featured nanostructure of NiPd hNPs were well dispersed with a narrow size distribution. The average diameter of NiPd hNPs was 40 nm and the thickness of the alloy shell was about 5 nm. Dynamic light scattering analysis of NiPd hNPs was performed as shown in Fig. S1. Besides, EDX characterization of NiPd hNPs proved that their composition was metal Ni and Pd (Fig S2A). The Ni/Pd molar ratio was 0.84 measured by ICP-MS. XPS spectra of Pd 3d in NiPd hNPs were presented in the Fig. S2B. A pair of doublet peaks at 340.2 eV and 334.9 eV were both observed, revealing that Pd in NiPd hNPs is mostly metallic Pd (0) in the alloyed nanostructures.

To investigate the triple enzyme-like activity of NiPd hNPs, a series of experiments were carried out. NiPd hNPs could catalyze the fast oxidation of TMB, ABTS and OPD with the presence of H_2O_2 to give different colors as shown in Fig. 2A, indicating that NiPd hNPs possessed peroxidase-like activity.

Meanwhile, NiPd hNPs could also catalyze the direct oxidation of TMB to produce the typical blue color reaction in the absence of H_2O_2, suggesting the oxidase-like activity of NiPd hNPs (Fig. 2C). To further study the oxidation of TMB, the oxidizing agent (i.e. dissolved oxygen) in the reaction system (TMB-O_2-NiPd hNPs) was evaluated. A set of experiments were implemented as shown in Fig. 2C. The color of TMB was little changed when the system was bubbled with N_2 30 min while the absorbance at 652 nm of TMB oxidation increased obviously after saturation with O_2. It was found that the oxidase-like activity of NiPd hNPs could be improved by increasing oxygen concentration. The dissolved oxygen played an important role as the electron acceptor in the TMB oxidation reaction.

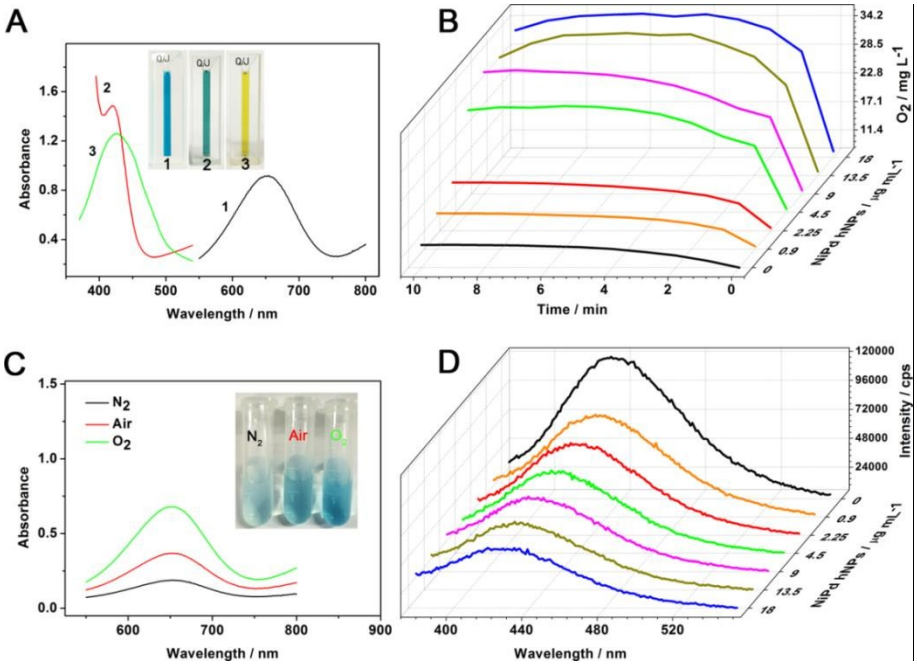

Fig. 2. (A) NiPd hNPs catalyze the oxidation of various substrates to produce different color reactions in the present of H_2O_2. (1) TMB, (2) ABTS, (3) OPD. (B) Effect of the NiPd hNPs concentration on the O_2 generation from H_2O_2 decomposition. Reaction conditions: 50 mM H_2O_2 and different concentrations of NiPd hNPs were incubated in 0.1 M HAc-NaAc buffer (pH 5.0). (C) Effect of O_2 concentration on the direct oxidation of TMB by NiPd hNPs without any oxidizing agents. Reaction conditions: 0.25 mM TMB and 4.5 μg mL^{-1} NiPd hNPs were incubated in 0.1 M HAc-NaAc buffer (pH 5.0) for 5 min for absorbance spectroscopy measurement. The NaAc buffer was bubbled with N_2 or O_2 for 30 min. (D) The effect of NiPd hNPs on the formation of hydroxyl radical with terephthalic acid as a fluorescence probe.

Furthermore, intrinsic catalase-like activity was also exhibited in NiPd hNPs, which could catalyze the decomposition of H_2O_2 to generate oxygen. To test the catalase-like activity of NiPd hNPs, a dissolved oxygen meter was employed to measure the oxygen generation from the H_2O_2 decomposition in a NiPd hNPs concentration-dependent manner. From Fig. 2B, it could be observed that oxygen concentration increased as the increase of NiPd hNPs. This indicated that NiPd hNPs possessed the catalase-like activity.

According to the above phenomena, we assume that the catalysis mechanism with respect to triple enzyme-like NiPd hNPs may result from the formation of •OH during the reactions. To verify this hypothesis, the •OH intensity in H_2O_2-NiPd hNPs system was determined via monitoring the fluorescence signal of 2-hydroxy terephthalic acid generated by the strong interaction between terephthalic acid and •OH radical.[14] Interestingly, the fluorescence intensity gradually decreased as the increase of NiPd hNPs (Fig. 2D), suggesting that NiPd hNPs could consume •OH radicals rather than generate ones. It should be noted that this phenomenon is similar with the behavior of the Co_3O_4 NPs reported.[15] Hence, the peroxidase-like activity of NiPd hNPs does not originate from generating •OH radical. On the other hand, the result suggested that NiPd hNPs could reduce the •OH production by catalyzing the composition of H_2O_2, which also provided a direct evidence that NiPd hNPs exhibited catalase-like activity.

To explore the role of each metal element on the triple-enzyme mimetic activity, Ni nanoparticles (Ni NPs) and Pd nanoparticles (Pd NPs) were obtained also by using $NaBH_4$ as a reducer and trisodium citrate as the stabilizing agent. Fig. S3 showed the TEM images of Ni NPs, Pd NPs and NiPd hNPs. The obtained Ni NPs had the similar size with NiPd hNPs while Pd NPs were the smallest among these three catalysts. To compare the triple-enzyme mimetic activity of each catalyst, serval experiments were conducted as shown in Fig. S4 and S5. It was found that Ni NPs could hardly catalyze oxidation of TMB even in the present of H_2O_2 and Ni NPs could not catalyze the decomposition of H_2O_2, either. On the other hand, Pd NPs possessed the triple-enzyme mimetic activity. But each kind of enzyme mimetic activity was lower than that of NiPd NPs in the same reaction conditions. According to these results, we could conclude that the triple-enzyme mimetic activity of NiPd hNPs was owing to the metal Pd. Meta Ni also played an indispensable role of improving the enzyme-like catalytic activity even if no obvious enzyme-like catalytic behaviours could be observed with respect to Ni NPs. With metal Ni, NiPd hNPs possessed the hollow-featured nanostructure, which could provide a large surface area with active sites for the catalytic reaction and increase the collision probability of the active molecules when TMB and H_2O_2 were trapped in the hollow nanoparticles, leading to the high catalytic activity of NiPd hNPs.

Further experiments were conducted to explore the peroxidase-like activity of NiPd hNPs. Similar to HRP, the catalytic activity of NiPd hNPs was depended on the pH, temperature and H_2O_2 concentration. The peroxidase-like activity of NiPd hNPs was measured by varying the pH from 2 to 10 and the temperature from 20 °C to 55 °C. Fig. S6 showed that the catalytic activity of NiPd hNPs was much higher in weakly acidic solution than in neutral or basic solution, as had been reported for peroxidase-like NPs and HRP.[7a, 11, 16] The maximum catalytic activity was obtained under the condition of pH 5.0 and 40 °C. For simplicity, we adopted the optimized condition of pH 5.0 and room temperature (~20 °C) for subsequent analysis of NiPd hNPs activity.

The apparent steady-state kinetic parameters for this reaction were determined by changing the concentration of TMB and H_2O_2 in the system, respectively. The value ε = 39 000 $M^{-1}cm^{-1}$ (at 652 nm) for the oxidized product of TMB was used

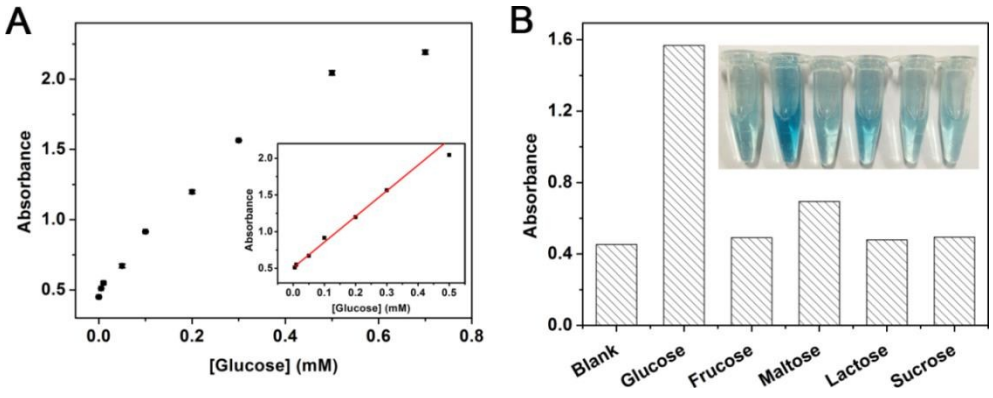

Fig. 3. (A) Dose-response curve for glucose detection at 652 nm. Inset shows their respective linear calibration plots. The error bars represents the standard deviation of three parallel measurements. (B) Determination of the selectivity of glucose detection (from left to right: blank, 0.3 mM glucose, 3 mM fructose, 3 mM maltose, 3 mM lactose and 3 mM sucrose). Inset: the color change with the different solutions.

here to obtain the corresponding concentration term from the absorbance data. Typical Michaelis-Menten curves were observed in Fig. S7. The maximum initial velocity (V_{max}) and Michaelis-Menten constant (K_m) given in Table S1 were calculated by using Lineweaver-Burk double-reciprocal plots (Fig. S7C and S7D). As we all know, the K_m value of enzyme is a crucial parameter to measure the affinity for the substrates. Lower K_m value means higher affinity. From Table S1, NiPd hNPs (K_m = 0.11 mM) were found possessing much higher affinity for TMB than that of HRP (K_m = 0.434 mM). On the other hand, the K_m value with H_2O_2 as substrate was 0.66 mM, which was about 6 times lower than that of HRP, suggesting that a lower H_2O_2 concentration was required for the NiPd hNPs when the maximum activity was obtained. Compared with other Pd-based catalysts showed in Table S1, NiPd hNPs also exhibited remarkable affinity for TMB and H_2O_2.

As shown in Fig. S8, the reproducibility among five batches of NiPd hNPs and long-term repeatability were investigated. The relative standard deviation (RSD) was 5.3% for five batches of NiPd hNPs, implying the excellent reproducibility of peroxidase activity of NiPd hNPs. After two month, the catalytic activity could maintain above 90%, showing their high stability during long-term storage. These advantages would broaden their applications in the field of biomedicine and bioassay.

On the basis of the intrinsic peroxidase-like activity of NiPd hNPs, a simple TMB colorimetric method was developed by combining GOD with NiPd hNPs to detect glucose. As presented in Fig. 3A, the absorbance was linearly correlated to glucose concentration from 0.005 mM to 0.5 mM with a detection limit of 4.2 μM, which was comparative to the conventional methods as shown in table S2. Based on colorimetric method, this glucose biosensor also gave lower LODs than that using other nanomaterials as a catalyst. To test the selectivity for glucose detection, fructose, maltose, lactose and sucrose were chosen as control samples. Fig. 3B (the inset) shows that the color difference could be distinguished by naked eye even the concentration of control samples was 10 times larger than glucose, suggesting the high selectivity of the biosensing system for glucose detection. In addition, the analysis of glucose was carried out in 20-fold dilution urine samples and the results were listed in table S3. It can be seen that the recoveries of glucose fall in 98.0%–102.0% with the standard addition method, indicating that GOD-based colorimetric method is applicable to determine glucose in urine samples.

In summary, NiPd hNPs synthesized by galvanic replacement method exhibited triple-enzyme mimetic activity: oxidase-like activity, peroxidase-like activity and catalase-like activity. The peroxidase-like catalytic behavior of NiPd hNPs was analyzed in detail. As peroxidase mimic, NiPd hNPs were used to develop a new glucose biosensor with a limit of detection of 4.2 μM. The proposed biosensor showed high sensitivity and selectivity to glucose analysis. Furthermore, NiPd hNPs possessed excellent advantages like easy preparation, high stability and repeatability, which facilitate the utilization of peroxidase mimic in various fields, such as environmental chemistry, medical diagnostics and biotechnology.

This work is supported by the National Natural Science Foundation of China (No. 21375123) and the Ministry of Science and Technology of China (No. 2013YQ170585).

Notes and references

1 (a) H. Wei and E. Wang, *Chem. Soc. Rev.*, 2013, **42**, 6060; (b) R. Breslow, *Artificial Enzymes*, Wiley, 2006; (c) A. J. Kirby and F. Hollfelder, *From enzyme models to model enzymes*, Royal Society of Chemistry, 2009.
2 L. Gao, J. Zhuang, L. Nie, J. Zhang, Y. Zhang, N. Gu, T. Wang, J. Feng, D. Yang, S. Perrett and X. Yan, *Nat Nano*, 2007, **2**, 577.
3 E. Nakamura and H. Isobe, *Acc. Chem. Res.*, 2003, **36**, 807.
4 Y. Xiong, S. Chen, F. Ye, L. Su, C. Zhang, S. Shen and S. Zhao, *Chem. Commun.*, 2015, **51**, 4635.
5 L. Su, W. Qin, H. Zhang, Z. U. Rahman, C. Ren, S. Ma and X. Chen, *Biosens. Bioelectron.*, 2015, **63**, 384.
6 Y. Li, X. He, J.-J. Yin, Y. Ma, P. Zhang, J. Li, Y. Ding, J. Zhang, Y. Zhao, Z. Chai and Z. Zhang, *Angew. Chem. Int. Ed.*, 2015, **54**, 1832.
7 (a) L. Zhang, L. Han, P. Hu, L. Wang and S. Dong, *Chem. Commun.*, 2013, **49**, 10480; (b) N. R. Nirala, S. Pandey, A. Bansal, V. K. Singh, B. Mukherjee, P. S. Saxena and A. Srivastava, *Biosensors & bioelectronics*, 2015, **74**, 207; (c) s. zhang, H. Li, Z. Y. Wang, J. Liu, H. Zhang, B. Wang and Z. Y. Yang, *Nanoscale*, 2015.
8 (a) S. Ge, W. Liu, H. Liu, F. Liu, J. Yu, M. Yan and J. Huang, *Biosens. Bioelectron.*, 2015, **71**, 456; (b) P. C. Pandey and R. Singh, *RSC Advances*, 2015, **5**, 10964; (c) G.-L. Wang, L.-Y. Jin, Y.-M. Dong, X.-M. Wu and Z.-J. Li, *Biosens. Bioelectron.*, 2015, **64**, 523; (d) Y. Tao, E. Ju, J. Ren and X. Qu, *Adv. Mater.*, 2015, **27**, 1097; (e) T. Wen, W. He, Y. Chong, Y. Liu, J.-J. Yin and X. Wu, *PCCP*, 2015; (f) C. M. Maroneze, G. P. dos Santos, V. B. de Moraes, L. P. da Costa and L. T. Kubota, *Biosens. Bioelectron.*
9 J. Xi, Y. Zhang, N. Wang, L. Wang, Z. Zhang, F. Xiao and S. Wang, *ACS Appl. Mat. Interfaces*, 2015, **7**, 5583.
10 (a) X. Zheng, Q. Zhu, H. Song, X. Zhao, T. Yi, H. Chen and X. Chen, *ACS Appl. Mat. Interfaces*, 2015, **7**, 3480; (b) M. Liu, H. Zhao, S. Chen, H. Yu and X. Quan, *ACS Nano*, 2012, **6**, 3142.
11 X. Xia, J. Zhang, N. Lu, M. J. Kim, K. Ghale, Y. Xu, E. McKenzie, J. Liu and H. Yet, *Acs Nano*, 2015, **9**, 9994.
12 (a) J. Y. Chen, B. Wiley, J. McLellan, Y. J. Xiong, Z. Y. Li and Y. N. Xia, *Nano Lett.*, 2005, **5**, 2058; (b) X. Teng, Q. Wang, P. Liu, W. Han, A. I. Frenkel, Wen, N. Marinkovic, J. C. Hanson and J. A. Rodriguez, *J. Am. Chem. Soc.*, 2008, **130**, 1093; (c) L. Chen, H. Guo, T. Fujita, A. Hirata, W. Zhang, A. Inoue and M. Chen, *Adv. Funct. Mater.*, 2011, **21**, 4364.
13 M. Wang, W. Zhang, J. Wang, D. Wexler, S. D. Poynton, R. C. T. Slade, H. Liu, B. Winther-Jensen, R. Kerr, D. Shi and J. Chen, *ACS Appl. Mat. Interfaces*, 2013, **5**, 12708.
14 K.-i. Ishibashi, A. Fujishima, T. Watanabe and K. Hashimoto, *J. Photochem. Photobiol., A*, 2000, **134**, 139.
15 J. Mu, Y. Wang, M. Zhao and L. Zhang, *Chem. Commun.*, 2012, **48**, 2540.
16 L. Gao, J. Zhuang, L. Nie, J. Zhang, Y. Zhang, N. Gu, T. Wang, J. Feng, D. Yang and S. Perrett, *Nat. Nanotechnol.*, 2007, **2**, 577.